












# Journal of the Geological Survey of Brazil

## Fragments of juvenile Siderian continental crust in the Rio Piranhas-Seridó Domain, Borborema Province, Northeastern Brazil, as deduced by zircon U-Pb and whole-rock Sm-Nd systematics

Alan Pereira da Costa<sup>1\*</sup> , Rogério Cavalcante<sup>1</sup> , Alexandre Ranier Dantas<sup>1</sup> , Joseneusa Brilhante Rodrigues<sup>2</sup> , André Luiz Carneiro da Cunha<sup>3</sup> , Geysson de Almeida Lages<sup>3</sup> , Vanja Coelho Alcântara<sup>3</sup> , Rafael Bittencourt Lima<sup>4</sup> , André Luís Spisila<sup>5</sup> 

<sup>1</sup>CPRM-Serviço Geológico do Brasil (NANA/SUREG-RE), Rua Professor Antônio Henrique de Melo, 2010, Natal, RN, Brazil, CEP: 59078-580

<sup>2</sup>CPRM-Serviço Geológico do Brasil (SEDE), Setor Bancário Norte - SBN Quadra 02, Bloco H - Asa Norte, Brasília, DF, Brazil, CEP: 70040-904

<sup>3</sup>CPRM-Serviço Geológico do Brasil (SUREG-RE), Av. Sul, 2291, Recife, PE, Brazil, CEP:50770-011.

<sup>4</sup>CPRM-Serviço Geológico do Brasil (GEREMI/SUREG-SP), Rua Costa 55, Consolação, São Paulo, SP, Brazil, CEP 01304-010.

<sup>5</sup>CPRM-Serviço Geológico do Brasil (NUBA/SUREG-SP) Rua Voluntários da Pátria, 475, 1º andar cj. 10, Curitiba, PR, Brazil, CEP: 80020-926.

### Abstract

In the Rio Piranhas-Seridó Domain (PSD), Borborema Province, geological mapping and aerogammaspectrometric data, combined with studies of Sm-Nd isotopes in whole rock and U-Pb in tonalitic orthogneiss and metamorphic clinopyroxene-hornblendite zircons enabled the identification and individualization of geological units with crystallization ages of  $2456 \pm 4$  Ma and  $2381 \pm 16$  Ma, respectively (U-Pb in zircon). These Siderian rocks are part of the basement of the central and northern portions of the PSD and are called the Arabia Complex. The tonalitic orthogneiss has an Sm-Nd (TDM) model age of 2.56 Ga, with an  $\epsilon_{Nd}$  value of +1.20, which allows inferring a juvenile source for the magma that gave rise to the protoliths of the rocks from the Arabia Complex. The identification and improvement of the geological cartography of Siderian units in the central portion of the PSD has contributed to a better understanding of the events of juvenile crust generation for the Borborema Province in general and inserts the province in the worldwide debate on geotectonic evolution during the Siderian Period.

### Article Information

Publication type: Research Papers  
Received 2 June 2021  
Accepted 19 November 2021  
Online pub. 8 December 2021  
Editor: Evandro Klein

**Keywords:**  
Paleoproterozoic,  
Siderian,  
Basement,  
Crustal evolution,  
Juvenile crust,  
Borborema

\*\*Corresponding author  
Alan Pereira da Costa  
alan.costa@cprm.gov.br

### 1. Introduction

The Siderian Period (2.5 to 2.3 Ga) of the Paleoproterozoic era has been the target of intense debate in the world's geological literature because there is no consensus about its geotectonic evolution. Lines of research advocate the existence of an apparent tectonic calm-stagnation (shutdown by Condie et al. 2009 or tectono-magmatic Lull by Spencer et al. 2018), while other lines of research argue that this period, in fact, is not so calm in comparison to the processes that generate juvenile crusts (Pehrsson et al. 2014). The use of new tools into regional geological mapping, e.g., aerogeophysical data from gamma spectrometry combined with the popularization and refinement of geochronological (U-Pb) and isotopic (Sm-Nd) methods, has promoted, in recent years, significant

advances in the cartographic individualization of geological units other than those already known in the Borborema Province.

In the Borborema Province, in northeastern Brazil (Figure 1), rocks from the Siderian age, mostly composed of TTG-type gneisses, are reported in the Middle-Coreaú Domain (Santos et al. 2009); they compose part of the Granjeiro Complex (Hollanda et al. 2015; Pitarello et al. 2019) and locally in the Alto Moxotó Domain (Melo et al. 2002; Santos et al. 2013, Santos et al. 2015, 2017; Brito Neves et al. 2020). Rocks from the Siderian age have not yet been well documented from a cartographic point of view so far in the central portion of the Rio Piranhas-Seridó Domain (PSD). So far, the existing geological descriptions in the literature have treated its basement as formed mainly by gneisses and migmatites of



diverse compositions, with ages ranging from the Riacian to the Orosirian (Hackspacher et al. 1990; Legrand et al. 1991; Dantas et al. 2007; Hollanda et al. 2011; Costa and Dantas 2014; Souza et al. 2016). Neoarchean and Paleoproterozoic ages have also been described for rocks that compose the PSD basement (Oliveira et al. 2013; Costa et al. 2018; Santos et al. 2020; Cavalcante et al. 2019; Ferreira et al. 2020a; 2020b).

The present study presents geological, geophysical, isotopic and geochronological integration data, which allowed the individualization of geological units from the Siderian age (one of which was proven to be juvenile) in two areas located in the central part of the PSD. This documentation of juvenile Siderian rocks in the PSD contributes to a better understanding of this period in Borborema, as well as as in other areas of Brazil, such as the Bacajá Domain in the Amazon Craton (Vasquez et al. 2008) and the Mineiro Belt in the São Francisco Craton (Seixas et al. 2012).

## 2. Regional Geological Context

This study was carried out in the northern portion of the Borborema Province (Ebert 1970; Almeida et al. 1981), northeast of Brazil (Fig. 1). This province is composed of a complex mosaic of rocks that underwent a tectonic evolution related to a collage of lithospheric fragments from Archean and Paleoproterozoic ages surrounded by sequences of metasedimentary rocks. Such fragments belong mainly to the São Francisco/Congo and São Luis/West African cratons (Trompette 1994; Brito Neves et al. 2002; Cordani et al. 2003). In the final stage of evolution, the Brasiliano orogeny outlined the current structure of the Borborema Province, clearly marked by the establishment of transient shear zones associated with high-volume Ediacaran plutonic activity (Brito Neves 1975; Almeida et al. 1981; Santos and Brito Neves 1984; Jardim de Sá 1994; Vauchez et al. 1995; Neves et al. 1996; Archanjo et al. 1999; Brito Neves et al. 2000). According to Caxito (2013) the geological evolution of the Borborema Province is particularly based on two main hypotheses: (i) in the first, its crust would have grown in complete tectonic cycles with crustal rifting, opening and closing of oceans, establishment of subduction and continental collision zones (Santos 1996; Brito Neves et al. 2000; Medeiros 2004); (ii) in the second, it would have been formed by a single continental block with a stable Archean-Paleoproterozoic basement since 2.0 Ga, with establishment followed by an inversion of the ensialic basins on the basement (Neves 2003; Neves et al. 2006).

The tectonic subdivision of the province is based on terrain models and/or tectonostratigraphic domains (e.g., Almeida et al. 1976; Brito Neves, 1983; Santos and Brito Neves, 1984; Jardim de Sá et al. 1992; Santos 1996; Jardim de Sá 1994; Van Schmus et al. 1995; Brito Neves et al. 2000; Santos et al. 2000; Medeiros 2004; Medeiros et al. 2017, 2021) and its boundaries are established by faults and regional shear zones. In this study, we use the subdivision proposed by Medeiros et al. (2017, 2021), which divides the province into nine domains: Middle Coreaú, Central Ceará, Jaguaribeano, Piranhas-Seridó River, São José do Campestre, Transversal Zone, Pernambuco-Alagoas, Sergipano and Riacho do Pontal (Fig. 1).

In relation to this subdivision, the areas investigated in this study are located in the central portion of the Piranhas-Seridó Domain River (PSD), which would be delimited to the south, east and west, respectively, by the Patos, Picuí-João Câmara

and Portalegre shear zones, while the northern limit of this domain is covered by Phanerozoic covers of the Potiguar Basin (Fig. 1).

The PSD is described as a domain constituted by a crystalline basement predominantly from the Riacian/Orosian age, containing Archean remnants (Oliveira et al. 2013; Costa et al. 2019; Santos et al. 2020; Cavalcante et al. 2018, 2019; Medeiros et al. 2021). The set of these units occurs is partially capped by Neoproterozoic metasupracrustal rocks from the Seridó Group (Jucurutu, Ecuador and Seridó formations, Van Schmus et al. 2003), all of which are intruded by Brazilian igneous bodies, in addition to dikes and Mesozoic and Cenozoic volcanic plugs (Figure 1).

The main geological and geochronological studies carried out on the PSD basement rocks between 1980 and 2000 indicated that the generation of rocks with U-Pb ages ranged between 2.2 and 2.1 Ga (Table 1). These rocks were gathered in the Caicó Complex (Hackspacher et al. 1990; Dantas 1992; Jardim de Sá 1994), whose major constitution is given by orthogneisses of different compositions (sometimes with augen textures), migmatitic gneisses, banded gneisses, metamafic and metaltramafic rocks, paragneisses, paraderivative shales and marbles.

The first pieces of evidence of older rocks for the basement of the PSD were proposed by Negrão et al. (2005) based on isotopic studies by the Sm-Nd method, with ages found of model T ages DM ranging from 2.97 Ga to 3.88 Ga. Later, Dantas et al. (2008) based on U-Pb zircon determinations, identified Siderian ages of  $2336 \pm 12$  Ma in a calcisilicate rock intercalated with amphibolites and  $2331 \pm 37$  Ma in a tonalitic biotite-hornblende gneiss, including these rocks in the Santa Luzia Sequence. In the same region addressed by Negrão et al. (2005) and Dantas et al. (2008), Costa and Dantas (2014) individualized and mapped a Siderian age unit, naming it the Arabia Complex instead of the Santa Luzia Sequence proposed by Dantas et al. (2008), owing to issues relative to the stratigraphic nomenclature code, since the term sequence does not apply to the designation of formal units.

## 3. Analytical procedures

The samples used in the U-Pb and Sm-Nd petrographic and isotopic studies were collected during the geological mapping work carried out in two areas of the PSD, Area I, north of the domain, and Area II, center of the domain (Fig. 1), with the aid of aerogeophysical data from gamma spectrometry collected by CPRM in the Paraíba-Rio Grande do Norte Aerogeophysical Project (LASA SA and Prospectors 2010). This project surveyed high-resolution aeromagnetic and aerogammaspectrometric profiles, with flight and control lines spaced 500 m and 5,000 m apart, oriented in the NS and EW directions, respectively, with the flight height set at 100 meters over the ground.

The U-Pb geochronological zircon data were collected from three samples from the two study areas: AP-242B (orthogneiss - Area I); AP-01C (amphibolite - Area II); and AP-02 (metamorphic clinopyroxene-hornblende - Area II). The samples were prepared in the petrography laboratory of the CPRM (Regional Superintendence of Recife) according to the following steps: (i) crushing of approximately 10 kg of each sample with a reduction to the fraction <2 cm; (ii) milling (Mineral Technology Laboratory of the Department of

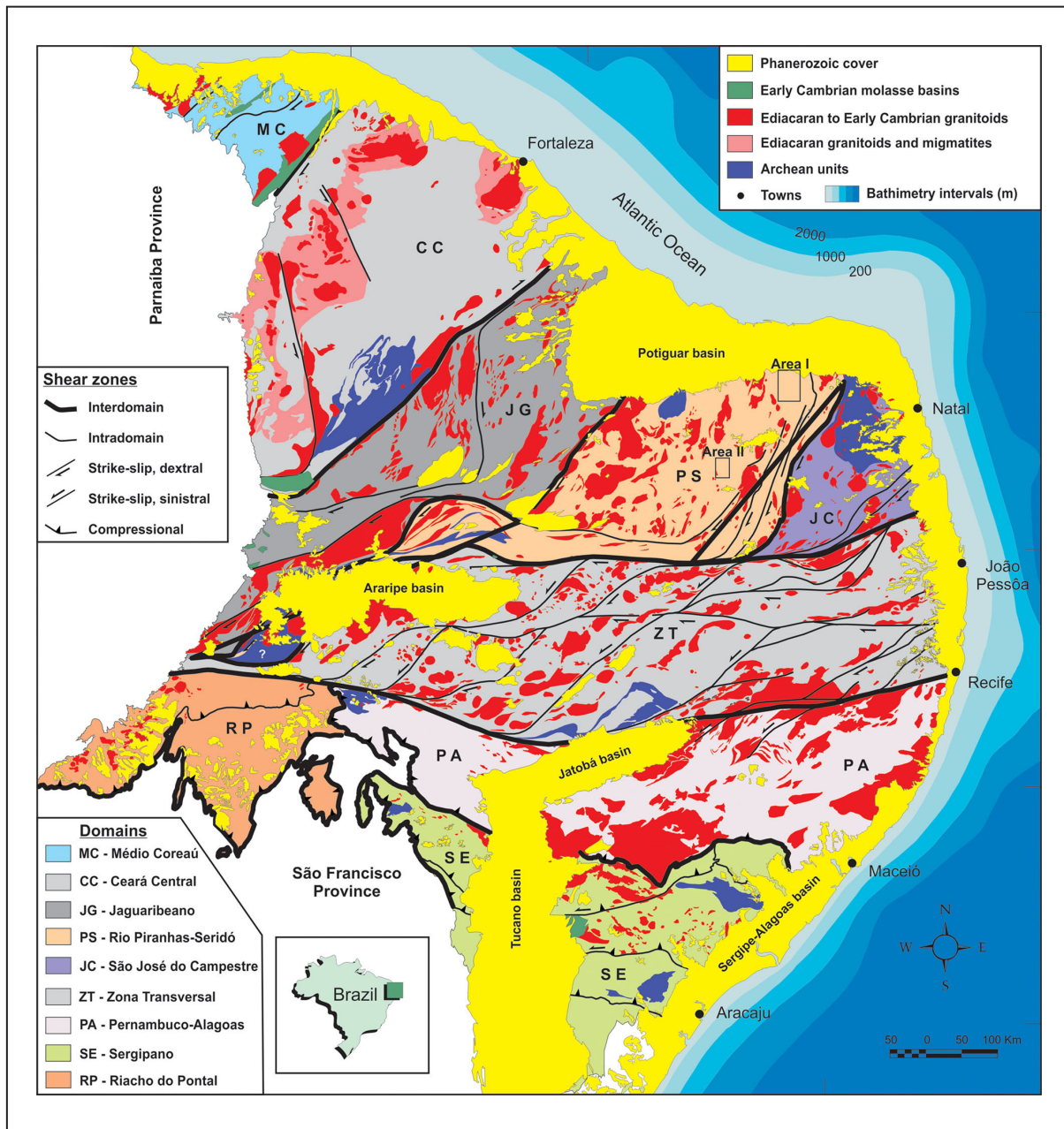


**FIGURE 1.** Location and geological compartmentation of the Borborema Province; the study areas in the Piranhas-Seridó River Domain (PSD) are highlighted (Medeiros et al., 2021).

Mining Engineering, UFPE); (iii) drying the ground sample in an oven at a temperature of 80°C; (iv) sieving to collect the grains that pass through the 100 mesh sieve and are retained in the 170 mesh sieve; (v) gravimetric separation with heavy liquids; (vi) magnetic separation in a FRANTZ isodynamic separator; (vii) separation of the zircon crystals with the aid of a magnifying glass.

The U-Pb zircon isotope analysis of the AP-242B sample was performed in an ionic microprobe at the High Resolution Geochronology Laboratory, located at the University of São Paulo (USP), using the SHRIMP IIe/MC model. The zircon concentrates were mounted in epoxy resin at the Research Center in Geochronology and Isotopic Geochemistry (CPGeo/USP), where the assemblies were imaged by cathodoluminescence (CL) in a Scanning Electron Microscope (SEM).

The acquisition of isotopic data was performed with a 24  $\mu\text{m}$  primary electron beam. The concentration of U-Pb-Th was normalized using the international standard of zircon SL13 (238 ppm) and the  $^{206}\text{Pb}/^{238}\text{U}$  ratio was bracketed using the Temora 2 natural standard, aged 416.78 Ma (Black et al. 2004). Secondary pattern analyses (Z6266 -  $566 \pm 4$  Ma, Stern & Amelin, 2003) were used to measure accuracy. The analysis conditions were: 6 scans, dead time = 25 ns and source slit = 80  $\mu\text{m}$ . For data reduction, the Squid 1.06 program (Ludwig 2002) was used.

Samples AP-02 and AP-01C were analyzed via LA-ICPMS at the Geochronological Research Center (University of São Paulo) and at the Geochronology Laboratory (Federal University of Ouro Preto, UFOP), respectively. The internal structure of the zircon crystals of these samples was investigated using electron backscattered images (BSE)

**TABLE 1** – Summary of the main Paleoproterozoic ages (U-Pb zircon) published for the basement rocks of the Rio Piranhas-Seridó Domain

Age (Ma)	Error (Ma)	Rock type	Locality (State*)	Reference
2156	5.6	Biotite granodiorite	Florânia (RN)	Hackspacher et al., (1990)
2146	4.4	Biotite orthogneiss	Florânia (RN)	Hackspacher et al., (1990)
2151	7.6	Metagabbro	Florânia (RN)	Hackspacher et al., (1990)
2242	6	Granodiorite	Caicó (RN)	Legrand et al., (1991)
2181	10	Tonalitic orthogneiss	Assu (RN)	Souza et al., (2007)
2198	13	Metahornblendite	São Vicente (RN)	Nascimento et al., (2011)
2207	35	Metagabbro	Currais Novos (RN)	Hollanda et al., (2011)
2248	18	Augen gneiss	São José do Seridó (RN)	Hollanda et al., (2011)
2208	13	Leucogneiss	Santana do Matos (RN)	Hollanda et al., (2011)
2172	24	Augen gneiss	Antônio Martins (RN)	Hollanda et al., (2011)
2234	7.3	Augen gneiss	Lajes (RN)	Costa e Dantas (2014)
2150	18	Metandesite	Assu (RN)	Souza et al., (2016)
2225	13	Granodiorite orthogneiss	Caicó (RN)	Souza et al., (2016)
2113	15	Granite sheet	Caicó (RN)	Souza et al., (2016)
2336	12	Calc-silicate rock	Pedro Avelino (RN)	Dantas et al. (2008)
2331	37	Tonalitic gneiss	Pedro Avelino (RN)	Dantas et al. (2008)
2400	40	Banded felsic gneiss	Junco do Seridó (PB)	Hollanda et al., (2011)
2456	4	Granodiorite orthogneiss	Pedro Avelino (RN)	Costa e Dantas (2014)
2356	12	Biotite gneiss	Lavras de Mangabeira (CE)	Freimann (2014)
2367	12	Amphibolite	Lavras de Mangabeira (CE)	Freimann (2014)
2461	30	Metaquartz-diorite	Ipaumirim (CE)	Ancelmi (2016)
2479	15	Diorite orthogneiss	Farias de Brito (CE)	Palheta et al., (2019)
2370	21	Amphibolite	Granjeiro (CE)	Palheta et al., (2019)

\* RN – Rio Grande do Norte, PB – Paraíba, CE – Ceará

from a SEM (FEI, Quanta 450) at CPRM in Brasília, under conditions of 20 kV, about 100  $\mu$ A. In both laboratories the ratios were determined between isotopes  $^{202}\text{Hg}$ ,  $^{204}(\text{Pb}+\text{Hg})$ ,  $^{206}\text{Pb}$ ,  $^{207}\text{Pb}$ ,  $^{208}\text{Pb}$ ,  $^{232}\text{Th}$  and  $^{238}\text{U}$ .

At UFOP, the analyses were performed using the ICP-MS Element 2 spectrometer, a thermo-Finnigan magnetic sector monocollector model, coupled to an Excimer M50 193 nm laser system. Grain ablation was performed in 30  $\mu$ m spots. In all analyses, the BB international standard (Santos et al. 2017) was used to correct the equipment's drift, as well as the fractionation between the U and Pb isotopes. Accuracy was checked through analyses performed using the GJ-1 standard, 608.5 $\pm$ 1.5 Ma (Jackson et al. 2004). Data were acquired in *peak jumping* mode for 20s of background, followed by 20s of sample ablation. Raw data reduction, which includes fixes for *background*, derived from the equipment and common lead, was performed by the Glitter® software.

The analyses carried out at USP used a LA-MC-ICP-MS Neptune device (Thermo-Finnigan) coupled to the ArF Excimer laser ( $\lambda=193\text{nm}$ , Photon Machines). The ablation conditions were: 32- $\mu$ m spot, frequency of 6 Hz and fluence of about 6 mJ of intensity. Acquisition took place in 50 cycles of 1 second each. The analytical sequence was 2 blanks, 3 GJ-1 standards, 12 samples, 2 blanks and 3 GJ-1 standards. Accuracy was controlled through various analyses in the international Mud Tank standard (Black and Gulson 1978). Data reduction was performed in a spreadsheet developed in the laboratory and includes blank correction, equipment drift and common lead correction.

The calculations for all ages and the generation of graphs were performed in Excel® with the resources of the ISOPLOT

4.15 supplement from the Berkeley Geochronology Center (Ludwig 2012).

The sample AP-242B was analyzed by the Sm-Nd method in whole rock at the Geochronology Laboratory of the University of Brasília (UnB), following the methodology described by Gioia and Pimentel (2000). In this procedure, about 50 mg of powdered sample was mixed with a tracer solution of  $^{149}\text{Sm}$  and  $^{150}\text{Nd}$ . The sample was dissolved in Savillex® capsules through successive acid attacks on HF, HNO<sub>3</sub> and HCl. The Sm and Nd contents were extracted through cation exchange columns, made in Teflon and filled with LN-Spec resin. The Sm and Nd salts were deposited on rhenium filaments with nitric acid and evaporated. The readings of the ratios were carried out in a Finnigan MAT 262 mass spectrometer in static mode. The  $^{143}\text{Nd}/^{144}\text{Nd}$  ratio was normalized on the basis of the  $^{146}\text{Nd}/^{144}\text{Nd}$  ratio of 0.7219. The value of TDM was calculated using the model of De Paolo (1981), using the ISOPLOT 4.15 software (Ludwig, 2012). The uncertainties for the  $^{147}\text{Sm}/^{144}\text{Nd}$  e  $^{143}\text{Nd}/^{144}\text{Nd}$  ratios are less than  $\pm 0.5\%$  ( $2\sigma$ ) and  $\pm 0.005\%$  ( $2\sigma$ ), respectively, based on repeated analyses in international standards BHVO-1 and BCR-1.

## 4. Results

### 4.1. Petrography of the Arabia Complex

The rocks that compose the Arabia Complex were identified in two work areas, I and II (Figures 1, 2). Area I is located in the northern portion of the Piranhas-Seridó River Domain between the municipalities of Lajes and Pedro Avelino, while Area II is located in the central portion of this same domain, around the Ferro de Saquinho deposit, in the municipality of Cruzeta.

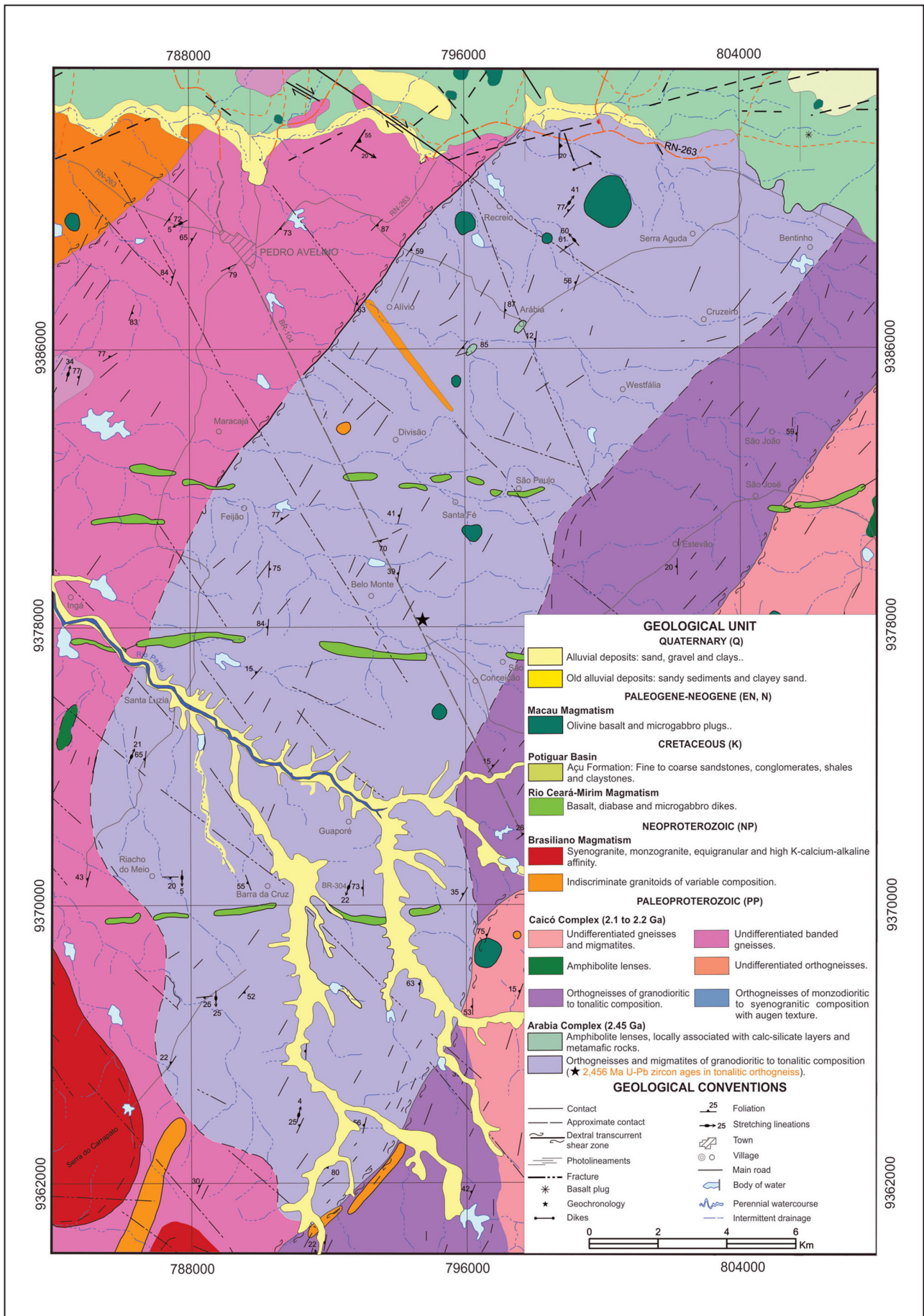


FIGURE 2. Geological map of Area I showing the geological contours of the Arabia Complex.

In Area I, the rocks that form the Arabia Complex are predominantly composed of orthogneisses and migmatitic, leucocratic, medium to coarse inequigranular gneisses with granodioritic to tonalitic composition, sometimes monzogranitic (Figures 3 A, B). There are also lenses and metric bodies of fine to medium textured amphibolites, embedded in orthoderived rocks (Figure 3C), or in the form of centimeter to metric xenoliths in orthoderived rocks of this complex (Figure 3D).

The gneisses have a banded, gneissic texture, with alternating inequigranular, granoblastic, elongated, fine-to-medium-grained felsic bands and fine-to-medium lepid-nematoblastic mafic bands, both with minerals whose size ranged between (>1 and 3mm). Its essential mineralogical composition includes quartz (20%), microcline (20%) and plagioclase (40%), and the main mafic minerals are biotite (7%) and hornblende (10%), and as accessories (3%) there are opaque minerals, apatite, titanite, zircon, allanite and epidote (Figure 4 A, B). Taking the QAP modal values, recalculating them to 100% and projecting them onto a QAP classificatory diagram for plutonic rocks (according to the IUGS recommendations, based on Streckeisen, 1976), we obtain  $Q=25.00\% + A= 25.00\% + P=50.00\%$ , which are projected in the compositional field of granodiorites.

In order to perform the geological interpretation and correlation of the gamma spectrometric data, the ternary composition (RGB) of the three radioelements potassium (K), thorium equivalent (eTh) and uranium equivalent (eU) was

used; there was differentiation radiometric between the rocks from Area I. The composition allowed the individualization of the rocks that compose the Arabia Complex from the other adjacent orthogneissic rocks, which are correlated to the Caicó Complex. Ternary composition data (RGB) (Figure 5A) show that, in relation to the Caicó Complex, the Arabia Complex in its southern and central portions is enriched in K, while eU and eTh are predominant in the northern portion (Figure 5 B, C, D).

In Area II, around the Saquinho iron deposit (Figures 2, 6), there are bodies of metamorphic clinopyroxene-hornblendite. These bodies are elongated, sometimes intercalated with felsic gneisses (Figure 7) and spatially associated with lenses and amphibolite bodies from the Caicó Complex (Figure 6).

Micropetrographic data show a rock with a granonematoblastic, fine to coarse inequigranular, serial and non-oriented texture. The rock was originally pyroxenite, submitted to retrometamorphism, i.e., pyroxenes were hydrated and replaced by hornblende. Retrometamorphism also caused the instability of the hornblende, which, in turn, was replaced with actinolite, and it was classified as actinolitic hornblende.

Mineralogically, it is formed essentially by actinolitic hornblende (80%) and clinopyroxene (diopside-hedenbergite) (15%) while the other minerals (5%) are titanite, opaque minerals and allanite (Figure 8 A, B). The rock is classified as metamorphic clinopyroxene-hornblendite.

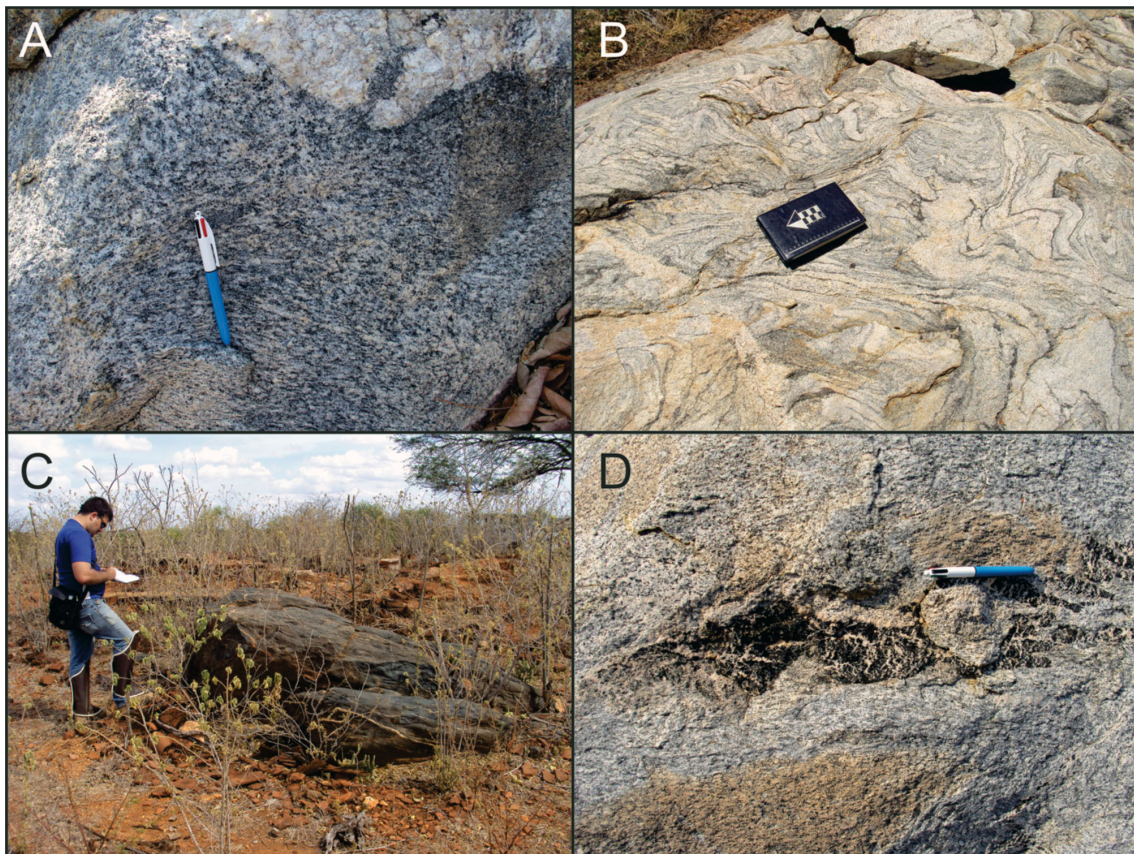


**FIGURE 3.** Images of rocks from the Arabia Complex. (A) Biotite amphibole orthogneiss granodiorite with discrete portions of fusion or nebulitic texture; (B) Migmatite diatextite with fold structure (AP-300 outcrop); (C) Amphibolite lens embedded in Arabia Complex orthogneisses (outcrop AP-262); (D) "Schlieren" of amphibolite xenolith in orthogneiss with the Arabia Complex (outcrop AP-242).

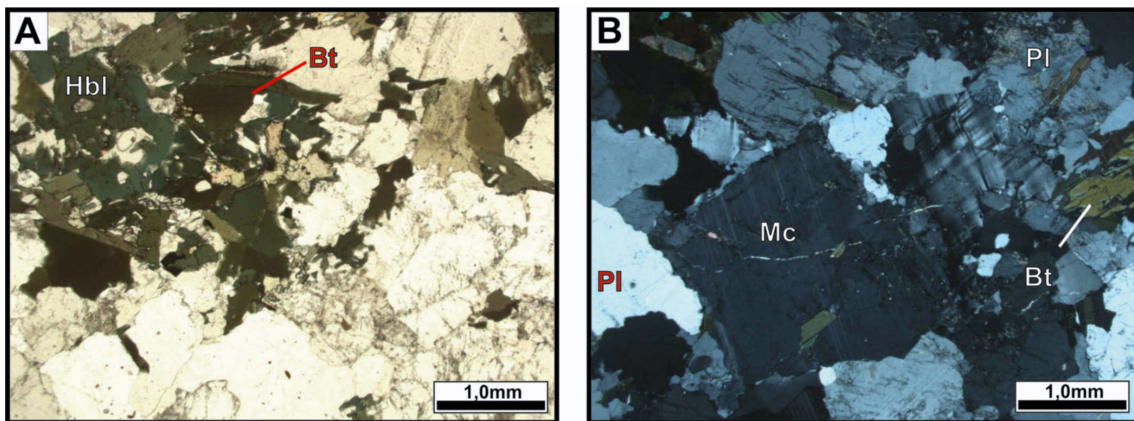


FIGURE 4. Micropetrographic aspects of the biotite-amphibole orthogneiss from the Arabia Complex dated in this study. (A) Parallel Nicols, (B) Parallel Nicols. Mc: microcline, Bt: biotite, Pl: plagioclase, Hbl hornblende.

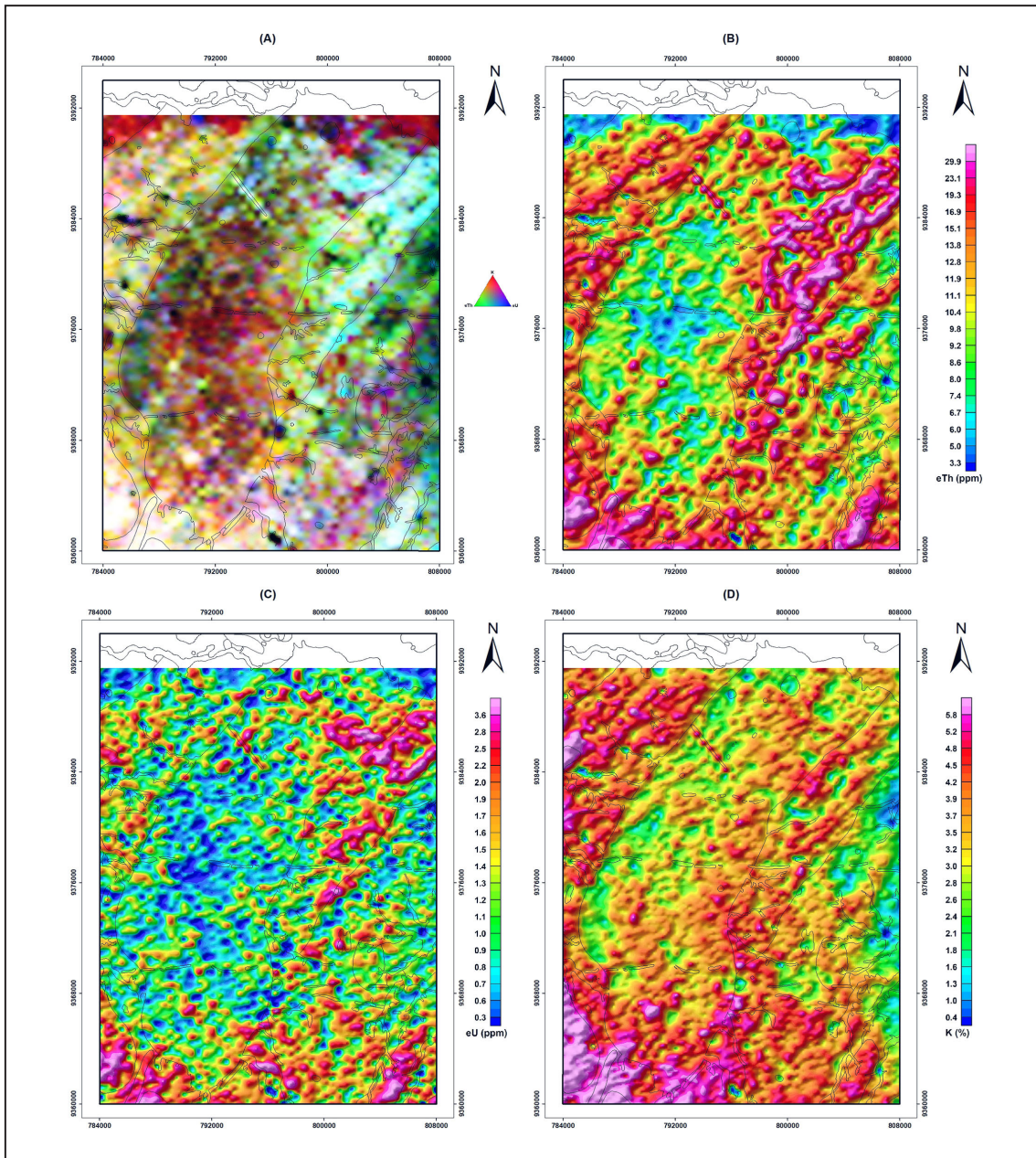


FIGURE 5. Aerogamaspectrometric maps of Area I with the boundaries of the mapped geological units. (A) RGB ternary composition; (B) eTh channel; (C) eU channel; (D) K channel.

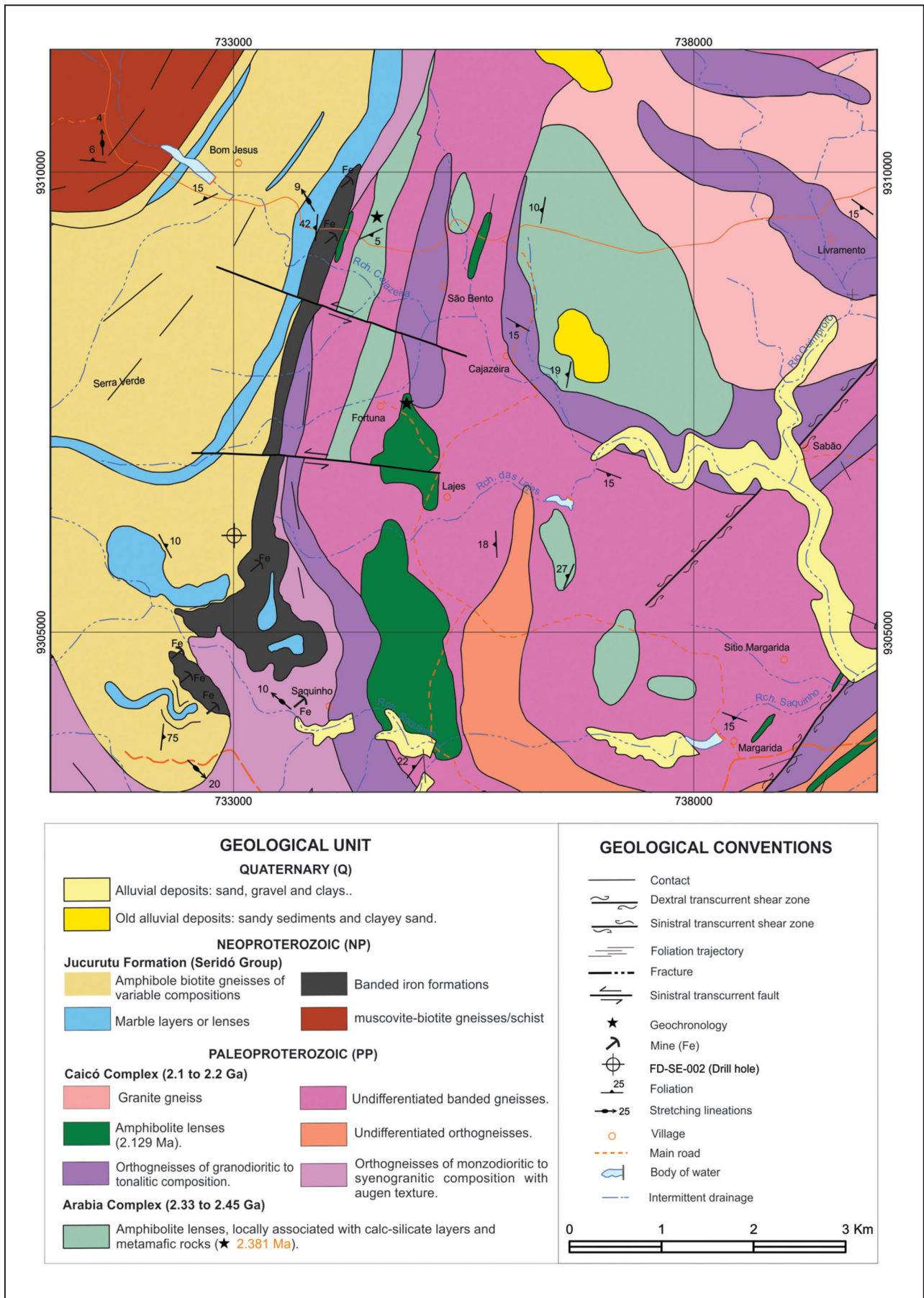


FIGURE 6. Geological map of Area II, in the Saquinho iron deposit region (Cavalcante et al. 2018), with emphasis on the mafic-ultramafic units of the Arabia Complex that occur among the orthogneiss, migmatites and amphibolites of the Caicó Complex.





FIGURE 7. Outcrop showing centimetric intercalations of mafic rock (metahornblendite) and felsic gneisses in low-angle foliation.

scattered and age could not be calculated. The Th/U ratios of these points were in the order of 0.30, a little smaller than those found in the nuclei. It can be interpreted that the age of  $2456 \pm 4$  Ma represents the crystallization age of the gneiss igneous protolith and that the superposed metamorphic event disturbed the system, but was not able to generate the isotopic rebalance of the mineral.

The same orthogneiss sample was analyzed using the Sm-Nd technique. The contents of Sm and Nd were relatively low (6.063 and 32.574 ppm, respectively) and showed a  $^{147}\text{Sm}/^{144}\text{Nd}$  of ratio 0.1125, within the expected range for felsic rocks. This result, in association with the  $^{143}\text{Nd}/^{144}\text{Nd}$  ratio of  $0.511339 \pm 0.000017$ , indicates the age model TDM of 2.56 Ga and  $\epsilon_{\text{Nd}}(t=2.46 \text{ Ga})$  of +1.20, which allows inferring a juvenile source for the magma generating the igneous protolith or gneiss.

For Area II, two samples were dated for U-Pb via LA-ICP-MS. Sample AP-01C is an amphibolite from the Caicó complex, dark green in color, with no apparent structure (Figure 11). This rock has large zircon crystals (150-350  $\mu\text{m}$ ),

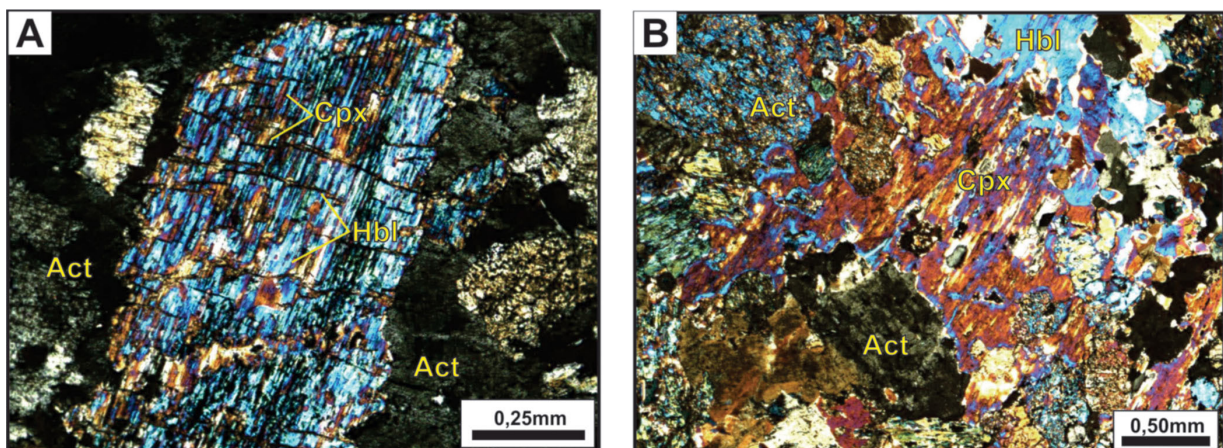


FIGURE 8. Micropetrographic aspects of the mineral assemblage that compose the metamafic rocks represented by metamorphic clinopyroxene-hornblendite from the Siderian ages that occur in Area II: In (A) and (B), the nicols are crossed. Act: actinolite, Cpx: clinopyroxene, Hbl: hornblende.

#### 4.2. U-Pb in zircon and Sm-Nd in whole rock

A sample (AP-242B) of biotite-amphibole orthogneiss (Figure 9) from Area I was analyzed (SHRIMP). Zircon crystals are small to large (30 to 300  $\mu\text{m}$ ), colorless, translucent to transparent bipyramidal prisms. In a cathodoluminescence image, one can see a complex internal structure (Figure 10a), with the presence of nuclei and edges. Oscillatory zoning is the most frequent feature, although edges, recesses and chaotic texture can be identified. U-Pb isotopic composition was determined in fifteen points in eleven crystals (Table 2). Eleven out of fifteen points were located in crystals without borders or in nuclei (main group), while the other four points were located in more homogeneous areas, suspected of being regrowth borders. The main group had Th/U ratios between 0.52 and 0.83 and a coherent set of  $^{207}\text{Pb}/^{235}\text{U}$  and  $^{206}\text{Pb}/^{238}\text{U}$  ratios. The most concordant data (9 points) allowed the calculation of the concordant age of  $2456 \pm 4$  Ma, with an MSWD value of 2.0 and a probability of concordance of 0.15 (Figure 10b). The isotopic data obtained at the edges were very



FIGURE 9. Sample AP-242B (biotite-amphibole orthogneiss) belonging to the Arabia Complex, analyzed by U-Pb (SHRIMP) and Sm-Nd (UTM: 9378166 and 794692, South Zone 24).

TABLE 2 - Isotopic data of U-Pb SHRIMP determinations in zircon from biotite-amphibole orthogneiss from the Arabia Complex.

Spot	f(206)%	U (ppm)	Th	<sup>232</sup> Th <sup>238</sup> U	Ratio*							Age* (Ma)					Remark
					<sup>207</sup> Pb*		%		<sup>206</sup> Pb*		err	<sup>206</sup> Pb	err	<sup>207</sup> Pb	err	% Disc.	
					<sup>206</sup> Pb	err	<sup>205</sup> U		<sup>238</sup> U	err							
1.1	0.03	256	129	0.52	0.16069	0.40	10.425	2.93	0.47055	2.9	0.99	2486	60	2463	7	-0.9	1
2.1	0.08	178	98	0.57	0.16090	0.53	9.889	3.06	0.44575	3.0	0.99	2376	60	2465	9	3.7	1
3.1	0.05	250	202	0.83	0.15997	0.43	10.319	2.93	0.46784	2.9	0.99	2474	60	2455	7	-0.8	1
3.2	0.05	177	60	0.35	0.13220	0.69	6.282	3.14	0.34464	3.1	0.98	1909	51	2127	12	11.4	3
4.1	0.04	161	90	0.58	0.16012	0.65	9.825	3.11	0.44502	3.0	0.98	2373	60	2457	11	3.5	1
5.1	0.12	165	83	0.52	0.15764	0.59	9.445	2.98	0.43454	2.9	0.98	2326	57	2431	10	4.5	2
5.2	0.08	247	40	0.17	0.12175	0.59	6.032	2.96	0.35931	2.9	0.98	1979	49	1982	11	0.2	3
6.1	0.10	155	91	0.61	0.15169	0.66	8.242	3.02	0.39406	2.9	0.98	2142	54	2365	11	10.4	2
6.2	0.05	206	45	0.22	0.15915	0.49	9.811	3.04	0.44709	3.0	0.99	2382	60	2447	8	2.7	1
7.1	0.11	162	100	0.63	0.16107	0.55	10.499	2.99	0.47278	2.9	0.98	2496	61	2467	9	-1.2	1
8.1	0.65	179	47	0.27	0.11558	1.34	5.197	3.24	0.32609	2.9	0.90	1819	46	1889	25	3.8	3
8.2	0.00	141	86	0.63	0.16054	0.57	10.589	3.01	0.47836	3.0	0.98	2520	62	2461	10	-2.3	1
9.1	0.06	246	130	0.54	0.15945	0.51	10.021	2.95	0.45584	2.9	0.98	2421	59	2450	9	1.2	1
10.1	0.04	221	149	0.70	0.15991	0.48	9.720	2.95	0.44086	2.9	0.99	2354	57	2455	8	4.3	1
11.1	0.00	370	109	0.31	0.14293	0.39	8.502	2.93	0.43140	2.9	0.99	2312	56	2263	7	-2.1	3

\*Ratios corrected for common lead based on the <sup>204</sup>Pb contents

Errors expressed as 1 sigma

f(206)% represents the common <sup>206</sup>Pb contents

1 - Spot used in age calculation

2 - Spot not used in age calculation

3 - Rims - Spot not used in age calculation

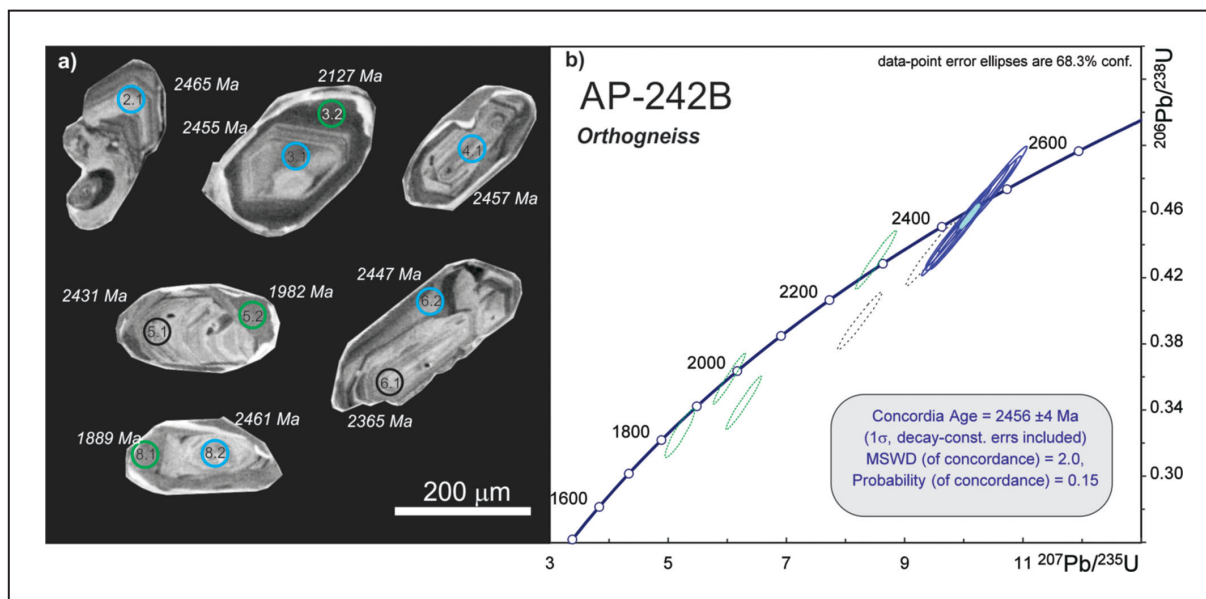


FIGURE 10. a) Cathodoluminescence image of zircon crystals from the AP-242B sample (biotite-amphibole orthogneiss from the Arabia Complex), with the identification of the crystal number and the <sup>207</sup>Pb/<sup>206</sup>Pb apparent age of the point shown in italics. The colors of the circles correspond to those used in the concord diagram. b) Concordia diagram for the SHRIMP data of sample AP-242B. Dashed lines indicate points that were not used for age calculation. Green dots represent isotopic data of the edges.

which are prisms, sometimes bipyramidal, and fragments. Most crystals are clear, but some have metamitic surfaces while others are heavily fractured. The BSE image shows crystals with a discrete oscillatory zoning, homogeneous crystals, crystals with a spongy texture and mixed crystals (Figure 12a). Owing to morphological diversity, 30 points in 27 crystals were analyzed (Table 3). The data are relatively dispersed along the concord (Figure 12b). A crystal showed <sup>207</sup>Pb/<sup>206</sup>Pb apparent age of 2453±20 Ma, much higher and

different from the others and therefore it is considered the result of crustal contamination. The main group of data, despite the dispersion, has similar behavior. Thus, their most concordant data were used to calculate the age of 2129 ± 52 Ma (Figure 12b), with MSWD of 0.31 and probability of agreement of 0.58. This result is interpreted as the crystallization age of the amphibolite protolith. The alignment of the other points in this group indicates loss of lead in the Neoproterozoic, but age could not be specified.

The second sample from Area II (AP-02) consists of a metamorphic clinopyroxene-hornblendite (Figure 13). The zircon crystals recovered from this sample are large prisms (150–250  $\mu\text{m}$ ) with little expressive bipyramid. They are clear crystals with few fractures and inclusions. The predominant internal structure in a BSE image (Figure 14a) is oscillatory zoning, although sectorial zoning and homogeneous edges could be seen some of them. Despite the morphological diversity, the isotopic data obtained at 24 points (from 20



FIGURE 11. Amphibolite (AP-01C) belonging to the Caicó Complex, dated by U-Pb (LA-ICP-MS) in zircon. (UTM: 9307513 and 734904, South Zone 24).

crystals) are similar (Table 3). The concord diagram (Figure 14b) shows agglomeration of data at about 2.4 Ga and some scattered points with reverse and normal disagreement. The selection of the most concordant points allowed the calculation of the age of  $2381 \pm 16$  Ma, with MSWD of 1.09 and probability of concordance of 0.30 (Figure 14b). This result is interpreted as the crystallization age of hornblendite.

## 5. Discussion and conclusions

The integration of geological, geophysical and isotopic data carried out in this study will allow a better understanding of the geological record during the Siderian period in two distinct areas of the Piranhas-Seridó Domain. In Area I (north of the domain), using geological cartography with the support of aerogeophysical data, an expressive portion of a fragment of juvenile continental crust of Siderian age could be individualized. It is found to be amalgamated between the Rhyacian rocks from the Caicó Complex. In Area II (center of the domain), the first evidence of the existence of older rocks for the crystalline basement came through U-Pb geochronological data carried out on subsurface rock samples (stratigraphic hole FD-SE-002 carried out by SGB - CPRM in 2014), which identified banded gneisses and Archean metamafic rocks (2512 Ma and 2501 Ma - Cavalcante et al. 2019). In an attempt to identify the outcropping presence of these rocks on the surface, this study identified a siderian rock (metamorphic clinopyroxene-hornblendite) with an age of  $2381 \pm 16$  Ma, which is here attributed to the Arabian Complex. This hornblendite is spatially associated with amphibolite bodies whose protolith has a crystallization age of  $2129 \pm 52$  Ma; thus, it can be correlated with the amphibolites from the Caicó Complex.

The ages determined in this study corroborate data reported by other authors (Souza et al. 2016), which indicate the presence of geological units of Siderian ages for the

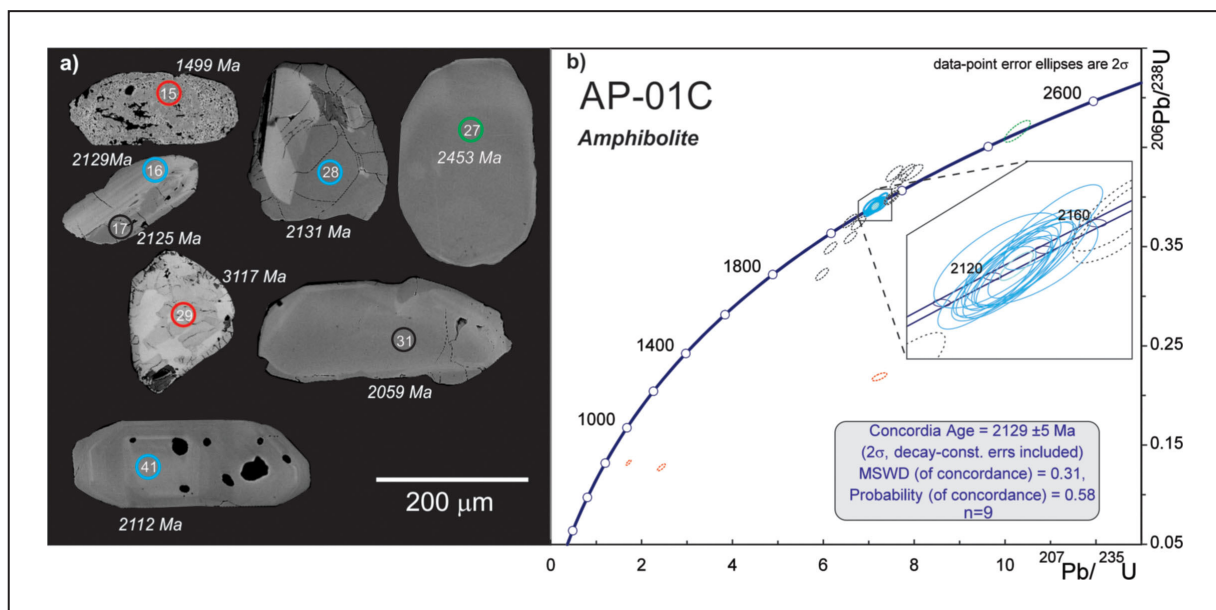


FIGURE 12. a) Electron backscattered image of zircon crystals from the AP-01C sample, with the identification of the crystal number and the  $^{207}\text{Pb}/^{206}\text{Pb}$  apparent ages in italics. The colors of the circles correspond to those used in the concord diagram. b) Concordia diagram for the LA-ICP-MS data of the AP-01C sample, belonging to the Caicó Complex. Dashed lines indicate points that were not used for age calculation. The green dots represent data interpreted as crustal contamination. The data with a high degree of disagreement are shown in red.



**FIGURE 13.** Outcrop with intercalation of mafic and felsic rock layers in which clinopyroxene-metahornblende was collected (sample AP-02) for U-Pb dating (LA-ICP-MS) in zircon. (UTM: 9309506 and 734542, South Zone 24).

crystalline basement of the PSD, which are about 250 Ma older than those that compose the Caicó Complex, which, according to data from the regional literature, show an age ranging between 2.2 and 2.1 Ga, thus corroborating the dating of the amphibolitic body of Area II.

Our U-Pb geochronological results, together with the Sm and Nd isotopic data, clearly indicate the existence of a Siderian juvenile event in the PSD, which needs to be looked into in more detail in further studies. The recognition of this juvenile Siderian continental crust for this portion of the Borborema Province corroborates data from the world literature that increasingly finds evidence of the action of geotectonic activity in this period in different cratons.

The results found in this reinforce the importance of carrying out geological mapping work combined with aerogeophysical data supported by geochronological (U-Pb) and isotopic (Sm-Nd, Lu-Hf) methods, even in areas with considerable prior geological knowledge. Similar studies should be carried out in other areas of the PSD to improve the geotectonic knowledge of the units that compose the crystalline basement in this domain.

**TABLE 3 -** Isotopic data of U-Pb determinations obtained via LA-MC-ICP-MS on zircon samples AP-01-C and AP-02.

Spot	f(206)%	U (ppm)	Th	Ratio								Age* (Ma)				% Disc.	Note
				<sup>232</sup> Th <sup>238</sup> U	<sup>207</sup> Pb* <sup>206</sup> Pb	% err	<sup>207</sup> Pb* <sup>235</sup> U	% err	<sup>206</sup> Pb* <sup>238</sup> U	% err	err	corr	<sup>206</sup> Pb err	<sup>207</sup> Pb err	<sup>206</sup> Pb err		
<b>AP-01C</b>																	
12	0.00	886	1193	1.35	0.13302	1.00	6.593	1.72	0.35945	1.40	0.81	2138	17	1980	24	7.4	1
13	0.01	340	244	0.72	0.13277	1.01	7.127	1.74	0.38934	1.41	0.81	2135	18	2120	26	0.7	2
14	0.00	749	956	1.28	0.13238	1.03	7.102	1.70	0.38912	1.35	0.79	2130	18	2119	24	0.5	2
15	0.00	583	263	0.45	0.09356	1.04	1.713	1.75	0.13277	1.42	0.81	1499	20	804	11	46.4	3
16	0.00	412	415	1.01	0.13233	1.10	7.098	1.81	0.38901	1.43	0.79	2129	19	2118	26	0.5	2
17	0.10	442	766	1.73	0.13431	1.02	5.968	1.74	0.32229	1.41	0.81	2155	18	1801	22	16.4	1
18	0.00	724	260	0.36	0.13312	1.04	7.214	1.82	0.39305	1.49	0.82	2140	18	2137	27	0.1	2
19	1.00	259	250	0.96	0.13303	1.82	7.189	2.35	0.39191	1.49	0.63	2138	32	2132	27	0.3	2
20	0.08	438	304	0.69	0.13149	1.01	6.778	1.73	0.37387	1.41	0.81	2118	18	2048	25	3.3	1
21	0.00	936	694	0.74	0.13543	1.02	7.470	1.68	0.40005	1.34	0.80	2170	18	2169	25	0.0	1
26	0.00	1434	449	0.31	0.13206	1.00	7.099	1.76	0.38987	1.45	0.82	2126	18	2122	26	0.2	2
27	0.00	30	31	1.07	0.15978	1.21	10.271	2.21	0.46623	1.85	0.84	2453	20	2467	38	-0.6	4
28	0.20	112	50	0.44	0.13248	1.14	7.160	2.04	0.39201	1.69	0.83	2131	20	2132	31	-0.1	2
29	0.02	2959	513	0.17	0.23958	1.00	7.235	1.72	0.21901	1.40	0.81	3117	16	1277	16	59.0	3
30	0.71	384	497	1.30	0.13832	1.46	2.435	2.32	0.12766	1.81	0.78	2206	25	775	13	64.9	3
31	0.00	64	79	1.24	0.12714	1.05	6.592	1.83	0.37604	1.50	0.82	2059	19	2058	26	0.1	1
32	0.04	353	402	1.14	0.12928	1.01	7.560	1.73	0.42412	1.41	0.81	2088	18	2279	27	-9.1	1
34	0.00	155	94	0.61	0.13194	1.06	7.050	1.77	0.38756	1.41	0.80	2124	19	2112	26	0.6	2
35	0.00	753	1178	1.56	0.13295	1.00	7.172	1.77	0.39127	1.46	0.83	2137	17	2129	27	0.4	2
40	0.00	333	260	0.78	0.13281	1.07	7.167	1.78	0.39137	1.42	0.80	2135	19	2129	26	0.3	2
41	0.75	44	29	0.66	0.13106	1.62	7.083	2.28	0.39198	1.61	0.71	2112	28	2132	29	-0.9	2
42	0.03	635	366	0.58	0.13345	1.01	7.836	1.72	0.42590	1.40	0.81	2144	18	2287	27	-6.7	1
43	0.00	242	224	0.92	0.13243	1.01	7.256	1.74	0.39736	1.42	0.81	2130	18	2157	26	-1.2	2
44	0.00	142	193	1.36	0.13327	1.01	7.646	1.76	0.41610	1.44	0.82	2141	18	2243	27	-4.7	1
45	0.00	522	546	1.05	0.13259	1.00	7.161	1.80	0.39169	1.50	0.83	2133	17	2131	27	0.1	2
46	0.04	839	330	0.39	0.13217	1.00	7.122	1.72	0.39080	1.40	0.81	2127	18	2127	25	0.0	2
47	0.00	635	257	0.40	0.12808	1.01	6.158	1.72	0.34870	1.40	0.81	2072	18	1928	23	6.9	1
48	1.00	1014	1154	1.14	0.13556	1.78	7.944	2.31	0.42503	1.47	0.64	2171	31	2283	28	-5.2	1
49	0.00	108	156	1.44	0.13615	1.13	7.493	1.91	0.39913	1.54	0.81	2179	20	2165	28	0.6	1

TABLE 3 - Isotopic data of U-Pb determinations obtained via LA-MC-ICP-MS on zircon samples AP-01-C and AP-02. (continued)

Spot	f(206)%	U (ppm)	Th	<sup>232</sup> Th <sup>238</sup> U	Ratio							Age* (Ma)				% Disc.	Note
					<sup>207</sup> Pb*	%	<sup>207</sup> Pb*	%	<sup>206</sup> Pb*	%	err	<sup>206</sup> Pb	err	<sup>207</sup> Pb	err		
					<sup>206</sup> Pb	err	<sup>235</sup> U	err	<sup>238</sup> U	err	corr	<sup>238</sup> U		<sup>206</sup> Pb			
<b>AP-02</b>																	
1.1	0.08	112	30	0.27	0.15580	2.57	9.691	2.60	0.45100	1.00	0.65	2400	20	2411	44	0.5	2
1.2	0.13	130	55	0.42	0.15530	2.77	9.549	2.72	0.44600	1.10	0.69	2378	22	2405	47	1.1	2
2.1	0.86	69	20	0.29	0.15830	3.22	9.909	3.09	0.45390	1.37	0.05	2413	27	2438	55	1.0	2
2.2	-0.42	-17	-3	0.19	0.14180	3.88	8.516	3.53	0.43550	1.70	0.64	2331	33	2249	65	-3.6	1
3.1	0.10	78	4	0.06	0.14170	3.18	8.076	3.39	0.41330	1.19	0.76	2230	22	2248	51	0.8	1
4.1	0.25	127	45	0.35	0.16190	2.66	10.177	2.69	0.45590	1.07	0.36	2421	21	2476	45	2.2	1
5.1	0.10	92	33	0.36	0.15380	2.73	9.370	2.73	0.44190	1.09	0.65	2359	21	2389	46	1.3	2
5.2	0.44	23	15	0.64	0.14830	3.10	9.765	3.02	0.47750	1.30	0.89	2516	27	2327	55	-8.1	1
6.1	0.03	189	31	0.16	0.15350	2.74	9.706	2.77	0.45850	1.07	0.62	2433	22	2385	46	-2.0	2
6.2	0.12	123	30	0.25	0.15920	2.95	10.198	2.86	0.46460	1.21	0.55	2460	25	2447	50	-0.5	1
7.1	0.37	25	13	0.50	0.15200	3.16	9.673	3.02	0.46140	1.30	0.88	2446	27	2369	54	-3.3	1
8.1	0.08	257	91	0.36	0.15380	2.54	9.086	2.63	0.42840	1.00	0.01	2298	19	2389	44	3.8	1
9.1	1.12	12	3	0.26	0.15400	2.08	9.552	2.01	0.45000	1.04	0.39	2395	21	2390	38	-0.2	2
10.1	0.05	201	38	0.19	0.15690	2.55	9.814	2.27	0.45350	1.21	0.94	2411	24	2423	42	0.5	2
11.1	0.10	133	69	0.52	0.15470	2.20	9.083	2.17	0.42590	1.08	0.86	2287	21	2398	36	4.6	1
12.1	0.16	144	47	0.33	0.15640	1.92	9.469	1.89	0.43920	0.93	0.01	2347	18	2417	33	2.9	1
13.1	0.15	74	29	0.39	0.14570	2.26	9.611	2.19	0.47840	1.07	0.53	2520	22	2296	41	-9.8	1
14.1	0.18	162	50	0.31	0.15300	2.22	9.390	2.09	0.44520	1.01	0.16	2374	20	2379	36	0.2	2
15.1	-9.95	2	-8	-5.21	0.15010	2.07	9.170	2.02	0.44310	0.99	0.01	2364	20	2347	35	-0.7	2
16.1	0.91	25	10	0.41	0.15410	2.01	9.461	1.97	0.44520	0.99	0.01	2374	20	2392	34	0.8	2
17.1	0.45	41	4	0.11	0.14540	2.54	8.816	2.21	0.43980	1.18	0.92	2350	24	2292	44	-2.5	2
18.1	0.03	274	1	0.00	0.12900	1.86	6.567	1.87	0.36940	0.89	0.70	2026	16	2084	33	2.8	1
19.1	0.05	227	65	0.29	0.13690	2.05	7.124	2.01	0.37730	1.01	0.01	2064	18	2189	35	5.7	1
20.1	0.13	96	25	0.26	0.15610	2.63	9.643	2.39	0.44790	1.29	0.82	2386	26	2414	45	1.2	2

\*Ratios corrected for common lead based on the <sup>204</sup>Pb contents

Errors expressed as 1 sigma

1 - Spot not used in age calculation

2 - Spot used in age calculation

3 - Discarded spot – highly discordant

4 - Crustal contamination

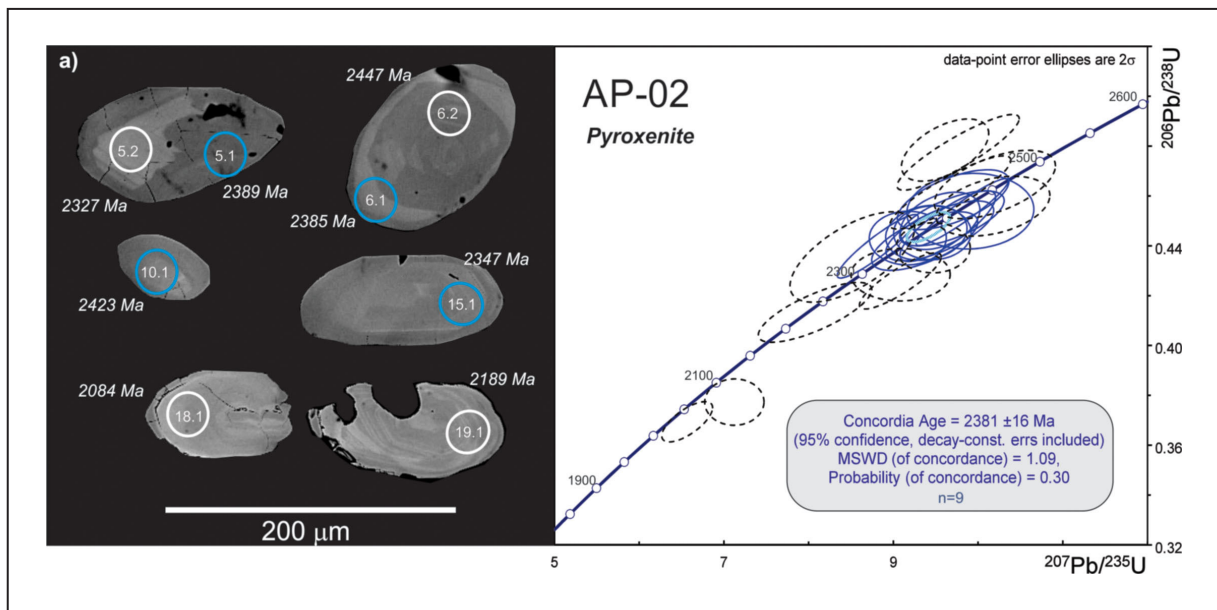


FIGURE 14. a) Electron backscattered image of zircon crystals from the AP-02 sample, with the identification of the crystal number and the <sup>207</sup>Pb/<sup>206</sup>Pb apparent ages in italics. The colors of the circles correspond to those used in the concordia diagram. b) Concordia diagram for the LA-ICP-MS data from the AP-02 sample. Dashed lines indicate points that were not used for age calculation.

## Acknowledgements

The authors acknowledge the comments of the two anonymous JGSB reviewers, which helped the improvement of the original manuscript.

## References

- Almeida F.F.M. et al. 1976. The upper Precambrian of South America. *Boletim IG/USP*, 7, 45-80. <http://www.ppegeo.igc.usp.br/index.php/bigusp/article/view/2088>
- Almeida F. F. M. et al. 1981. Brazilian structural provinces: an introduction. *Earth Sci. Rev.*, v.17, p.1- 29. [https://www.researchgate.net/publication/223838390\\_Brazilian\\_structural\\_provinces\\_An\\_introduction](https://www.researchgate.net/publication/223838390_Brazilian_structural_provinces_An_introduction)
- Ancelmi M.F. 2016. Geocronologia e geoquímica das rochas arqueanas do Complexo Granjeiro, Província Borborema. PhD Thesis, Instituto de Geociências, Universidade Estadual de Campinas, Campinas, 159 p. <http://repositorioslatinoamericanos.uchile.cl/handle/2250/1368031>
- Archanjo C.J. et al. 1999. Magnetic fabric and pluton emplacement in a transpressive shear zone system: The Itaporanga porphyritic granitic pluton (Northeast Brazil). *Tectonophysics*, 312, 331-345. [https://doi.org/10.1016/S0040-1951\(99\)00176-6](https://doi.org/10.1016/S0040-1951(99)00176-6)
- Black L.P., Gulson, B.L. 1978. The age of the Mud Tank Carbonatite, Strangways Range, Northern Territory. *B.M.R. J. Austral., Geol. Geophys.*, 3, 227-232. <https://data.gov.au/dataset/ds-ga-fae9173a-6fa1-71e4-e044-00144fdd4fa6/details?q=>
- Black L.P. et al. 2004. Improved 206Pb/238U microprobe geochronology by the monitoring of a trace-element-related matrix effect; SHRIMP, ID-TIMS, ELA-ICP-MS and oxygen isotope documentation for a series of zircon standards. *Chemical Geology*, 205, 115-140. <https://doi.org/10.1016/j.chemgeo.2004.01.003>
- Brito Neves B.B. 1975. Regionalização Geotectônica do Pré-Cambriano Nordeste. Tese de Doutorado, Instituto de Geociências, Universidade de São Paulo, São Paulo, 198 p. <https://teses.usp.br/teses/disponiveis/44/44132/tde-21062013-104857/pt-br.php>
- Brito Neves B.B. 1983. O mapa geológico do Nordeste oriental, escala 1:1.000.000. Tese de livre docência, Instituto de Geociências, Universidade de São Paulo, São Paulo, 177 p.
- Brito Neves B.B. et al. 2000. Tectonic history of the Borborema Province, Northeast Brazil. In: Cordani U.G. et al. (eds.). *Tectonic Evolution of South America*. Rio de Janeiro, 31 st International Geological Congress, 161-182. <https://rigeo.cprm.gov.br/handle/doc/19419>
- Brito Neves B.B. et al. 2002. North-western Africa - North-eastern Brazil. Major tectonic links and correlation problems. *Journal of African Earth Sciences*, 34, 275-278. <http://hdl.handle.net/11449/66860>
- Brito Neves B.B. et al. 2020. Alto Moxotó Terrane, a fragment of Columbia supercontinent in the Transversal Zone interior: Borborema Province, Northeast Brazil. *Brazilian Journal of Geology* 50, 2, 2020. <https://doi.org/10.1590/2317-4889202020190077>
- Cavalcante R. et al. 2019. Caracterização das rochas metamáficas-ultramáficas da região de Saquinho (Cruzeta/RN), Domínio Rio Piranhas-Seridó. In: *Simpósio de Geologia do Nordeste*, 28, p. 314.
- Cavalcante R. 2018. Neoproterozoic, Rhyacian and Neoproterozoic units of the Saquinho region, eastern Rio Piranhas-Seridó domain, Borborema Province (northeastern Brazil): implications for the stratigraphic model. *Journal of the Geological Survey of Brazil*. Brasília, 1, 1, 11-29. <https://doi.org/10.29396/jgsb.2018.v1.n1.2>
- Caxito F.A. 2013. Geotectônica e evolução crustal das Faixas Rio Preto e Riacho do Pontal, estados da Bahia, Pernambuco e Piauí. PhD Thesis, Universidade Federal de Minas Gerais, Belo Horizonte, 288 p. <https://repositorio.ufmg.br/handle/1843/IGCC-9DTEB9>
- Cordani U.G. et al. 2003. From Rodinia to Gondwana: a review of the available evidence from South America. *Gondwana Research*, 6, 2, 275-283. [https://doi.org/10.1016/S1342-937X\(05\)70976-X](https://doi.org/10.1016/S1342-937X(05)70976-X)
- Condie K.C. et al. 2009. Evidence and implications for a widespread magmatic shutdown for 250 My on Earth. *Earth and Planetary Science Letters*, 282, 294-298. [https://www.researchgate.net/publication/223745786\\_Evidence\\_and\\_implications\\_for\\_a\\_widespread\\_magmatic\\_shutdown\\_for\\_250\\_My\\_on\\_Earth](https://www.researchgate.net/publication/223745786_Evidence_and_implications_for_a_widespread_magmatic_shutdown_for_250_My_on_Earth)
- Costa A.P. et al. 2019. Projeto evolução crustal e metalogenia da província mineral do Seridó: folhas SB.24-Z-B-II-1 e SB.24-Z-B-II-3. Recife, CPRM. <https://rigeo.cprm.gov.br/jspui/handle/doc/17813>
- Costa A.P., Dantas A.R. 2018. Geologia e recursos minerais da folha Lajes SB.24-X-D-VI: estado do Rio Grande do Norte. Recife, CPRM. <http://rigeo.cprm.gov.br/jspui/handle/doc/20238>
- Costa A.P., Dantas A.R. 2014. Geologia e recursos minerais da folha Lajes SB.24-X-D-VI: estado do Rio Grande do Norte. Recife, CPRM. <http://rigeo.cprm.gov.br/jspui/handle/doc/20238>
- Dantas E.L. 1992. Evolução tectono-magmática do maciço polidiapírico São Vicente/Florânia – RN. MSc. Dissertation, Instituto de Geociências, Universidade Estadual Paulista Júlio Mequista Filho, Rio Claro, SP, 272 p.
- Dantas E.L. et al. 2008. 2,3 Ga continental crust generation in the Rio Grande do norte terrane, NE-Brazil. In: *South American Symposium on Isotope Geology*, 6, 40.
- De Paolo D.J. 1981. A neodymium and strontium isotopic study of the Mesozoic calc-alkaline granitic batholiths of the Sierra Nevada and Peninsular Ranges, California. *Journal of Geophysical Research*, 86, 10470-10488. [https://www.researchgate.net/publication/248788955\\_A\\_Neodymium\\_and\\_Strontium\\_Isotopic\\_Study\\_of\\_the\\_Mesozoic\\_Calc-Alkaline\\_Granitic\\_Batholiths\\_of\\_the\\_Sierra\\_Nevada\\_and\\_Peninsular\\_Ranges\\_California](https://www.researchgate.net/publication/248788955_A_Neodymium_and_Strontium_Isotopic_Study_of_the_Mesozoic_Calc-Alkaline_Granitic_Batholiths_of_the_Sierra_Nevada_and_Peninsular_Ranges_California)
- Ebert H. 1970. The Precambrian geology of the "Borborema"-Belt (States of Paraíba and Rio Grande do Norte; northeastern Brazil) and the origin of its mineral provinces. *Geologische Rundschau*, 59, 3, 1292-1326. <https://link.springer.com/article/10.1007/BF02042293>
- Ferreira A.C.D. et al. 2020a. Arc accretion and crustal reworking from late Archean to Neoproterozoic in Northeast Brazil. *Nature Communications*, 10, 1-12. <https://www.nature.com/articles/s41598-020-64688-9>
- Ferreira A.C.D. et al. 2020b. High-pressure metamorphic rocks in the Borborema Province, Northeast Brazil: Reworking of Archean oceanic crust during proterozoic orogenies. *Geoscience Frontiers*, 11, 2221-2242. <https://www.sciencedirect.com/science/article/pii/S1674987120300633>
- Freimann M.A. 2014. Geocronologia e petrografia de quartzos milonitos do duplex transcorrente de Lavras da Mangabeira. 2014. MSc Dissertation, Instituto de Geociências, Universidade de São Paulo, São Paulo, 2014, 83 p. <https://teses.usp.br/teses/disponiveis/44/44143/tde-26112014-144455/pt-br.php>
- Gioia S.M.C.L., Pimentel M.M. 2000. The Sm-Nd isotopic method in the Geochronology Laboratory of the University of Brasília. *Anais da Academia Brasileira de Ciências*, 72, 2, 219-245. <https://doi.org/10.1590/S0001-3765200000200009>
- Hackspacher P.C. et al. 1990. Um embasamento transamazônico na Província Borborema. In: *Congresso Brasileiro de Geologia*, 36, 2683-2696. <https://inis.iaea.org/collection/NCLCollectionStore/Public/22/070/22070962.pdf?r=1>
- Hollanda M.H.B.M. et al. 2011. Long-lived Paleoproterozoic granitic magmatism in the Seridó-Jaguaribe domain, Borborema Province-NE Brazil. *Journal of South American Earth Sciences*, 32, 4, 287-300. <https://doi.org/10.1016/j.jsames.2011.02.008>
- Hollanda M.H.B.M. et al. 2015. Detrital zircon ages and Nd isotope compositions of the Seridó and Lavras da Mangabeira basins (Borborema Province, NE Brazil): Evidence for exhumation and recycling associated with a major shift in sedimentary provenance. *Precamb. Res.*, 258, 186-207. <https://doi.org/10.1016/j.precamres.2014.12.009>
- Jackson S.E. et al. 2004. The application of laser ablation-inductively coupled plasma-mass spectrometry to in situ U-Pb zircon geochronology. *Chemical Geology*, 211, 47-69. <https://doi.org/10.1016/j.chemgeo.2004.06.017>
- Jardim de Sá E.F. 1994. A Faixa Seridó (Província Borborema, NE do Brasil) e o seu significado geodinâmico na Cadeia Brasileira/Pan-Africana. PhD Thesis, Universidade de Brasília, Brasília, 803 p. <http://mw.eco.br/ig/posg/dout/dout003.htm>
- Lasa Engenharia e Prospecções S.A., Prospectores Aerolevantamentos e Sistemas LTDA. 2010. Projeto Aero geofísico Paraíba-Rio Grande do Norte e Pernambuco-Paraíba. Rio de Janeiro, Lasa Engenharia e Prospecções S.A, 389 p.
- Legrand J.M. et al. 1991. Datação U/Pb e Rb/Sr das rochas precambrianas da região de Caicó. Reavaliação da definição de um embasamento arqueano. In: *Simpósio de Geologia do Nordeste*, 14, 276-279.
- Ludwig, K. 2002. SQUID Version 1.02 A User's Manual. Berkley Geochronological Center Special Publication, 2, 17 p.
- Ludwig K. 2012. User's manual for Isoplot version 3.75-4.15: a geochronological toolkit for Microsoft Excel. Berkley Geochronological

- Center Special Publication, 5.
- Medeiros V.C. 2004. Evolução geodinâmica e condicionamento estrutural dos terrenos Piancó-Alto Brígida e Alto Pajeú, Domínio da Zona Transversal, NE do Brasil. PhD Thesis, Universidade Federal do Rio Grande do Norte, Natal, 200 p. <https://rigeo.cprm.gov.br/handle/doc/105>
- Medeiros V.C. et al. 2017. O furo estratigráfico de Riacho Fechado (Currais Novos/RN), Domínio Rio Piranhas-Seridó (Província Borborema, NE Brasil): procedimentos e resultados. *Estudos Geológicos*, 27, 3, 3-44. <https://doi.org/10.18190/1980-8208/>
- Medeiros V.C. et al. 2021. The Rio Piranhas-Seridó Domain, Borborema Province, Northeastern Brazil: Review of geological-geochronological data and implications for stratigraphy and crustal evolution. *Journal of the Geological Survey of Brazil*, 4, 3. <https://doi.org/10.29396/jgsb.2021.v4.n3.1>.
- Melo O.O. et al. 2002. Idades U/Pb em zircão e idades modelo (Sm/Nd) de ortognaisses e enclaves metamórficos da área de Barro Vermelho-PE, terreno Alto Moxotó, Província Borborema, Nordeste do Brasil. *Revista Brasileira de Geociências* 32, 197–204. <http://dx.doi.org/10.25249/0375-7536.2002322197204>
- Nascimento M.A.L. et al. 2011. Integração de dados geocronológicos do Domínio Rio Piranhas - Seridó (RN-PB, NE do Brasil), com base em idades U-Pb. In: *Simpósio de Geologia do Nordeste*, 24, p. 391.
- Negrão M.N. et al. 2005. Evidências de Fontes Crustais Arqueanas na Região do Cabugi RN. In: *Simpósio de Geologia do Nordeste*, 21, p. 89.
- Neves S.P. 2003. Proterozoic history of the Borborema province (NE Brazil): Correlations with neighboring cratons and Pan-African belts and implications for the evolution of western Gondwana. *Tectonics*, 22, 1031. <https://doi.org/10.1029/2001TC001352>
- Neves S.P. et al. 1996. Shear-zone controlled magma emplacement or magma-assisted nucleation of shear zones? Insights from Northeast Brazil. *Tectonophysics*, 262, 349-365. [https://doi.org/10.1016/0040-1951\(96\)00007-8](https://doi.org/10.1016/0040-1951(96)00007-8)
- Neves S.P. et al. 2006. Timing of crust formation, deposition of supracrustal sequences, and Transamazonian and Brasiliano metamorphism in the East Pernambuco belt (Borborema Province, NE Brazil): implications for western Gondwana assembly. *Precambrian Research*, 149, 197–216. <http://dx.doi.org/10.1016/j.precamres.2006.06.005>
- Oliveira C.G. et al. 2013. Contribuição ao enquadramento metalogênico da Província Mineral do Seridó. *Seminário das Províncias Metalogênicas Brasileiras*, 1, p. 329-366.
- Palheta E.S.M. et al. 2019. Mapa geológico Granjeiro-Cococi, estado do Ceará. In: *Gomes I.P. 2021. Projeto Granjeiro Cococi*. Fortaleza, CPRM. <https://rigeo.cprm.gov.br/handle/doc/18691>
- Pehrsson S.J. et al. 2014. Did plate tectonics shutdown in the Paleoproterozoic? A view from the Siderian geologic record. *Gondwana Research*, 26, 3, 803-815. <http://dx.doi.org/10.1016/j.gr.2014.06.001>
- Pitarelo M.Z. et al. 2019. Syn-to post-depositional processes related to high grade metamorphic BIFs: Geochemical and geochronological evidences from a Paleo to Neoproterozoic (3.5–2.6 Ga) terrane in NE Brazil. *J. S. Am. Earth Sci.* 96, 102312. <http://dx.doi.org/10.1016/j.jsames.2019.102312>
- Santos E.J. et al. 1996. Ensaio preliminar sobre terrenos e tectônica acrescionária na Província Borborema. In: *Congresso Brasileiro de Geologia*, 39, 47-50. <http://www.sbgeo.org.br/home/pages/44>
- Santos E.J., Brito Neves B.B. 1984. Província Borborema. In: Almeida F.F.M., Hasui Y. (eds). *O Pré-Cambriano do Brasil*. São Paulo, Edgar Blucher Ltd., p. 123–186.
- Santos E.J. et al. 2000. An overall view on the displaced terrane arrangement of the Borborema Province, NE Brazil. In: *International Geological Congress*, 31. <https://repositorio.usp.br/item/001776711>
- Santos T.J.S. et al. 2009. Evidence for 2.35 to 2.30 Ga juvenile crustal growth in the northwest borborema Province, NE Brazil. *Geological Society, London, special Publications* 323, 271–281. <http://dx.doi.org/10.1144/SP323.13>
- Santos E.J. et al. 2013. The metacarbonate rocks of Itatuba (Paraíba): A record of sedimentary recycling in a Paleoproterozoic collision zone of the Borborema Province, NE Brazil. *Precamb. Res.*, 224, 454–471. <https://doi.org/10.1016/j.precamres.2012.09.021>
- Santos F.G. et al. 2020. Eo to Paleoproterozoic metamafic-ultramafic rocks from the central portion of the Rio Grande do Norte Domain, Borborema Province, northeast Brazil: The oldest South American platform rock. *Journal of South American Earth Sciences*, 97, 102410. <https://doi.org/10.1016/j.jsames.2019.102410>
- Santos L.C.M.L. et al. 2017. Neoproterozoic crustal growth and Paleoproterozoic reworking in the Borborema Province, NE Brazil: Insights from geochemical and isotopic data of TTG and metagranitic rocks of the Alto Moxotó Terrane. *J. S. Am. Earth Sci.* 79, 342–363. <https://doi.org/10.1016/j.jsames.2017.08.013>
- Santos, L.C.M.L. et al. 2015a. Early to late Paleoproterozoic magmatism in NE Brazil: The Alto Moxotó Terrane and its tectonic implications for the pre-West Gondwana assembly. *J. S. Am. Earth Sci.* 58, 188–209. <http://dx.doi.org/10.1016/j.jsames.2014.07.006>
- Santos M.M. et al. 2017. A New Appraisal of Sri Lankan BB Zircon as Reference Material for LA-ICP-MS U-Pb Geochronology and Lu-Hf Isotope Tracing. *Geostandards and Geoanalytical Research*, 41, 3, 335-358. <https://doi.org/10.1111/ggr.12167>
- Sato K. et al. 2014. Microsonda Iônica de Alta Resolução e de Alta Sensibilidade (SHRIMP IIe/MC) do Instituto de Geociências da Universidade de São Paulo, Brasil: método analítico e primeiros resultados. *Geologia USP, Série Científica*, 14, 3, 3-18. <http://dx.doi.org/10.5327/Z1519-874X201400030001>
- Seixas L.A.R. et al. 2012. Geochemistry, Nd isotopes and U-Pb geochronology of a 2350 Ma TTG suite, Minas Gerais, Brazil: implications for the crustal evolution of the southern São Francisco Craton. *Precambrian Research* 196, 61–80. <https://www.repositorio.ufop.br/handle/123456789/3930>
- Souza Z.S. et al. 2016. Generation of continental crust in the northern part of the Borborema Province, northeastern Brazil, from Archean to Neoproterozoic. *Journal of South American Earth Sciences*, 68, 68-96. <https://doi.org/10.1016/j.jsames.2015.10.006>
- Souza Z.S. et al. 2007. Calc-alkaline magmatism at the archaean e proterozoic transition: the Caicó complex basement (NE Brazil). *Journal of Petrology*, 48, 2149-2185. <https://academic.oup.com/petrology/article/48/11/2149/1566626>
- Souza Z.S. et al. et al. 2016. Generation of continental crust in the northern part of the Borborema Province, northeastern Brazil, from Archaean to Neoproterozoic. *Journal of South American Earth Sciences*, 68, 68-96. <https://doi.org/10.1016/j.jsames.2015.10.006>
- Spencer C.J. et al. 2018. A Palaeoproterozoic tectono-magmatic lull as a potential trigger for the supercontinent cycle. *Nature Geosciences*, 11, 97-101. <https://www.nature.com/articles/s41561-017-0051-y>
- Stern R.A., Amelin Y. 2003. Assessment of errors in SIMS zircon U-Pb geochronology using a natural zircon standard and NIST SRM 610 glass. *Chemical Geology*, 197, 1, 111-142. [https://doi.org/10.1016/S0009-2541\(02\)00320-0](https://doi.org/10.1016/S0009-2541(02)00320-0)
- Trompette R.R. et al. 1994. Geology of Western Gondwana (2000-500 Ma). Pan-African-Brasiliano aggregation of South America and Africa. London, CRC Press. 350 p. <https://doi.org/10.1201/9781003077664>.
- Van Schmus W.R. et al. 1995. U-Pb and Sm-Nd geochronologic studies of the Eastern Borborema Province, Northeast Brazil: initial conclusions. *Journal of South American Earth Sciences*, 8, 3-4, 267-288. [https://doi.org/10.1016/0895-9811\(95\)00013-6](https://doi.org/10.1016/0895-9811(95)00013-6)
- Van Schmus W.R. et al. 2003. The Seridó Group of NE Brazil, a late Neoproterozoic pré- to syncollisional basin in West Gondwana: insights from SHIRIMP U-Pb detrital zircons ages and Sm-Nd crustal residence (TDM) ages. *Precambrian Research*, 127, 287-386. [http://dx.doi.org/10.1016/S0301-9268\(03\)00197-9](http://dx.doi.org/10.1016/S0301-9268(03)00197-9)
- Vasquez M.L. et al. 2008a. Zircon geochronology of granitoids from the western Bacajá domain, southeastern Amazonian craton, Brazil: Neoproterozoic to Orosirian evolution. *Precambrian Research*, 161, 279-302. <http://dx.doi.org/10.1016/j.precamres.2007.09.001>
- Vauchez A. et al. 1995. The Borborema shear zone system, NE Brazil. *Journal of South American Earth Sciences*, 8, 3-4, 247-266. [https://doi.org/10.1016/0895-9811\(95\)00012-5](https://doi.org/10.1016/0895-9811(95)00012-5)